

Nonstationary Jammer Suppression Based on Parametric Sparse Reconstruction

Ben Wang^{*†}, Yimin D. Zhang[†], and Wei Wang^{*}

^{*}College of Automation, Harbin Engineering University, Harbin, 150001, China

[†]Department of Electrical and Computer Engineering, Temple University, Philadelphia, PA, 19122, USA

Abstract—We propose a nonstationary jammer signal suppression technique based on parametric sparse reconstruction, where sparsely sampled data are considered. By assuming nonstationary jammers that are characterized by polynomial phase signatures, a data-dependent parametric dictionary matrix is designed. In order to obtain an accurate instantaneous frequency estimation at a low computational complexity, we exploit an iterative multi-round sparse reconstruction scheme in which the dictionary matrix is updated with a finer grid size, thus leading to dictionary entries that are closer to the true jammer signatures. Simulation results are provided to verify the effectiveness of the proposed technique.

I. INTRODUCTION

Jammers suppression is an important problem in wireless communications, satellite navigation, and radio astronomy [1–5]. Recently, spectrum sharing between wireless communication, broadcast and other systems has also attracted strong research interests [6–9]. In this paper, we consider the situation where the desired signals are direct-sequence spectrum-spread (DS/SS) signals, which are commonly used in many wireless communication and satellite navigation systems, whereas the jammers assume popular nonstationary frequency modulated (FM) waveforms, such as linear FM and polynomial phase signals. In this case, conventional frequency-domain or time-domain jammer suppression techniques, such as notch filters and gating, become ineffective. Consider the fact that this kind of jammers are characterized by their instantaneous frequencies (IFs), anti-jam techniques can be developed based on the joint-variable signal representations to reveal the jammer signature in the time-frequency (TF) domain [10, 11]. In such approaches, the jammer excision process consists of two major steps [12]. In the first step, the TF representations of the received signals, which are dominated by the jammers, are obtained to estimate the jammer IF and phase signatures. In the second step, the jammer signals are removed based on the estimated IF and phase signatures with a minimum distortion to the desired signal. It is clear that the jammer mitigation

performance highly depends on the accuracy of estimated jammer IF and phase signatures.

Among various factors that limit and compromise the jammer IF estimation capability and performance, missing data samples generate a high level of artifacts that may significantly distort and obscure the jammer TF representations and thus degrade jammer IF estimation accuracy [13]. By exploiting the fact that nonstationary jammers are locally sparse in the TF domain due to their power localizations at and around their IFs, sparse representation based IF estimation algorithms have been proposed [13–16] and have found useful in anti-jam GPS receivers [12, 17–19]. However, these methods are based on non-parametric estimation of the jammer IF signatures which is sensitive to local distortions and missing data samples.

Note that the fact that most such smart jammers can be characterized as a polynomial phase signal over a short period of time. As such, we consider jammer phase estimation based on parametric sparse reconstruction in order to improve the jammer signature estimation and suppression performance. By discretizing the polynomial phase factors into a family of parameters, the desired data-dependent parametric dictionary matrix can be designed. Thus, the entries of the dictionary matrix contain the basis of the nonstationary jammers. In this case, the phase estimation is cast as a basis selecting problem. Accurate jammer phase estimation can be achieved if the grid size of the discretized factor set is sufficiently small. On the other hand, the dimension of the dictionary matrix has to be kept small in order to reduce the computational complexity. For this purpose, we exploit an iterative multi-round sparse reconstruction scheme in which the dictionary matrix is updated with a finer grid size, thus leading to dictionary entries that are closer to the true jammer signatures [20]. Simulation results verify that, when compared with the non-parametric sparse reconstruction counterpart [18], the proposed method achieves a higher TF resolution and is more robust to bursty missing samples.

Notations: We use lower-case (upper-case) bold characters to denote vectors (matrices). In particular, \mathbf{I}_N denotes the $N \times N$ identity matrix. $(\cdot)^*$ denotes complex conjugation, and $(\cdot)^T$ and $(\cdot)^H$, respectively, stand for transpose and Hermitian operations. $\delta(x)$ represents the Dirac delta function of x , \otimes denotes the Kronecker product, and $j = \sqrt{-1}$. In addition, $\|\cdot\|_1$ and $\|\cdot\|_2$ denote the ℓ_1 -norm and ℓ_2 -norm, respectively.

B. Wang is supported by the China Scholarship Council for his stay at the Temple University. The work of Y. D. Zhang is supported in part by the National Science Foundation under grant No. AST1547420. The work of W. Wang is supported by the National Natural Science Foundation (61571148), China Postdoctoral Special Funding (2015T80328), and China Postdoctoral Science Foundation Grant (2014M550182).

II. SIGNAL MODEL

We assume that Q_s DS/SS communication or navigation signals (referred to as desired signals hereafter) along with Q_j nonstationary FM jammers are received by a single-antenna receiver. The discrete-time received signal can be expressed as

$$x(t) = \sum_{i=1}^{Q_s} s_i(t) + \sum_{j=1}^{Q_j} s_j(t) + n(t), \quad (1)$$

where $t \in [0, \dots, G-1]$ denotes the time index, $s_i(t)$ and $s_j(t)$, respectively, denote the i th of desired signal and the j th nonstationary jammer with $i = 1, \dots, Q_s$ and $j = 1, \dots, Q_j$. In addition, $n(t)$ is the additive white Gaussian noise term with zero mean and variance σ_n^2 .

We model each jammer as a third-order polynomial signal. The IF signature of the j th jammer can be expressed in terms of the corresponding phase term as:

$$f_j(t) = \frac{1}{2\pi} \frac{d\varphi_j(t)}{dt} = a_j t^2 + b_j t + c_j, \quad (2)$$

where $\varphi_j(t)$ is the phase of the j th jammer signal, a_j , b_j and c_j are the polynomial coefficients.

Consider that the received signal is sampled at the Nyquist rate but with a high proportion of missing samples. The yielding sparse observations can be expressed as

$$y(t) = x(t) \cdot b(t), \quad (3)$$

where $b(t) \in \{0, 1\}$ is the observation mask. The index set of non-zero elements of $b(t)$ is denoted as \mathcal{S} with candidate $|\mathcal{S}| = N \leq G$.

III. JAMMER PHASE ESTIMATION BASED ON PARAMETRIC SPARSE RECONSTRUCTION

A. Parametric Sparse Reconstruction

Different from the TF based non-parametric sparse reconstruction techniques [12, 18], the proposed parametric approach designs the dictionary matrix depending on the polynomial phase coefficients of the jammer signals. These polynomial phase coefficients must be obtained during the estimation procedure. In comparison, non-parametric sparse reconstruction techniques do not consider the time-domain dependence in the dictionary matrix, which is usually an IDFT matrix independent of the signal arrivals.

Based on the IF signature presented in (2), the j th jammer signal in (1) can be further characterized as

$$s_j(t) = \alpha_j \exp\left(j2\pi\left(\frac{a^3}{3t^3} + \frac{b^3}{2t^2} + ct\right)\right), \quad (4)$$

with $\alpha_j = \beta_j e^{j\phi_j}$, where β_j and ϕ_j are the amplitude and initial phase of the j th jammer signal, respectively. The polynomial coefficients $\{a_j, b_j, c_j\}$ are selected from uniformly discretized coefficient sets, defined as row vectors, $\mathbf{a} = [\hat{a}_1, \dots, \hat{a}_K]$, $\mathbf{b} = [\hat{b}_1, \dots, \hat{b}_L]$ and $\mathbf{c} = [\hat{c}_1, \dots, \hat{c}_M]$, with respective step sizes Δa , Δb and Δc .

In practice, the pre-despreading desired signals have a much lower power compared with noise power, whereas the jammers are assumed to have a strong power because the use of DS/SS communication systems have a certain level of protection against weak jammers due to the spreading. Noting that the received signal is under sparse sampling, we denote the non-zero observations in (3) as $\bar{y}(t)$ with $t \in \mathcal{S}$. In this situation, the received signals can be expressed as

$$\bar{\mathbf{y}} = \Psi(\mathbf{a}, \mathbf{b}, \mathbf{c})\mathbf{r} + \bar{\mathbf{n}}, \quad (5)$$

where $\bar{\mathbf{y}} = [y(t_1), \dots, y(t_N)]^T \in \mathbb{C}^{N \times 1}$ is the non-zero observation vector with $t_m \in \mathcal{S}$, and $\Psi(\mathbf{a}, \mathbf{b}, \mathbf{c}) \in \mathbb{C}^{N \times (KLM)}$ is the parametric dictionary matrix with its element defined as

$$\Psi_{n, (k-1)LM + (l-1)M + m}(\mathbf{a}, \mathbf{b}, \mathbf{c}) = \exp\left(j2\pi\left(\frac{a_k}{3}t_n^3 + \frac{b_l}{2}t_n^2 + c_m t_n\right)\right),$$

with $a_k \in \mathbf{a}$, $b_l \in \mathbf{b}$, $c_m \in \mathbf{c}$. In addition, $\mathbf{r} \in \mathbb{C}^{KLM \times 1}$ is a sparse vector with an expected number of Q_j non-zero entries. The positions of these non-zero entries provide the information of the polynomial coefficients, whereas their values represent the estimates of $\alpha_1, \dots, \alpha_{Q_j}$. Furthermore, $\bar{\mathbf{n}} = [n(t_1), \dots, n(t_N)]^T$ is the noise vector.

Equation (5) is a standard compressive sensing formulation. Based on this formulation, we can obtain the phase of the jammers by solving the following ℓ_1 -norm minimization problem

$$\min \|\mathbf{r}\|_1 \quad \text{s.t.} \quad \|\bar{\mathbf{y}} - \Psi(\mathbf{a}, \mathbf{b}, \mathbf{c})\mathbf{r}\|_2^2 < \varepsilon, \quad (6)$$

where ε is a user-specific tolerance parameter. The ℓ_1 -norm minimization problem (6) can be solved by several methods, such as the orthogonal matching (OMP) [24], LASSO [25], Bayesian compressive sensing (BCS) [26, 27]. In this paper, the OMP algorithm is utilized to solve the above ℓ_1 -norm minimization problem in (6).

B. Multi-Round Sparse Reconstruction Scheme

It should be noted that, if the step sizes Δa , Δb and Δc are sufficiently small, the elements of the dictionary will be close to the true components of the jammer signals. In this case, an accurate IF estimation can be obtained. However, the dimension of the dictionary is proportional to the grid sizes of $(\mathbf{a}, \mathbf{b}, \mathbf{c})$ and, thereby, will lead to a high computational complexity in the recovery algorithm.

To reduce the complexity and, at the same time, guarantee the phase estimation accuracy, we propose the use of a multi-round CS algorithm. That is, we first design a dictionary matrix with relatively large step sizes $\Delta a^{(1)}$, $\Delta b^{(1)}$, $\Delta c^{(1)}$ to achieve a coarse estimation of the polynomial coefficients as the initial estimates. Then, we design the second dictionary matrix with a smaller step size $\Delta a^{(2)}$, $\Delta b^{(2)}$, $\Delta c^{(2)}$ around the initial estimates of $a_j^{(1)}$, $b_j^{(1)}$ and $c_j^{(1)}$ for $j = 1, \dots, Q_j$. Thus, in the second dictionary matrix, the polynomial coefficients can

be selected as $\mathbf{a}^{(2)} = [\tilde{\mathbf{a}}_1^{(2)}, \dots, \tilde{\mathbf{a}}_{Q_j}^{(2)}]$, $\mathbf{b}^{(2)} = [\tilde{\mathbf{b}}_1^{(2)}, \dots, \tilde{\mathbf{b}}_{Q_j}^{(2)}]$, $\mathbf{c}^{(2)} = [\tilde{\mathbf{c}}_1^{(2)}, \dots, \tilde{\mathbf{c}}_{Q_j}^{(2)}]$, where

$$\begin{aligned}\tilde{\mathbf{a}}_j^{(2)} &= \mathbf{a}_j^{(1)} + [-Z\Delta a^{(2)}, \dots, -\Delta a^{(2)}, 0, \Delta a^{(2)}, \dots, Z\Delta a^{(2)}], \\ \tilde{\mathbf{b}}_j^{(2)} &= \mathbf{b}_j^{(1)} + [-Z\Delta b^{(2)}, \dots, -\Delta b^{(2)}, 0, \Delta b^{(2)}, \dots, Z\Delta b^{(2)}], \\ \tilde{\mathbf{c}}_j^{(2)} &= \mathbf{c}_j^{(1)} + [-Z\Delta c^{(2)}, \dots, -\Delta c^{(2)}, 0, \Delta c^{(2)}, \dots, Z\Delta c^{(2)}],\end{aligned}$$

and Z determines the number of elements in each vector. Then, the entries of the dictionary matrix $\Psi(\mathbf{a}^{(2)}, \mathbf{b}^{(2)}, \mathbf{c}^{(2)}) \in \mathbb{C}^{N \times (2Z+1)^3}$ can be designed based on the coefficient set $(a_{m_1}, b_{m_2}, c_{m_3}) \in (\mathbf{a}^{(2)}, \mathbf{b}^{(2)}, \mathbf{c}^{(2)})$, i.e.,

$$\begin{aligned}\Psi_{n, (m_1-1)(2Z+1)^2 Q_j^2 + (m_2-1)(2Z+1)Q_j + m_3}(\mathbf{a}^{(2)}, \mathbf{b}^{(2)}, \mathbf{c}^{(2)}) \\ = \exp\left(j2\pi\left(\frac{a_{m_1}}{3}t_n^3 + \frac{b_{m_2}}{2}t_n^2 + c_{m_3}t_n\right)\right),\end{aligned}\quad (7)$$

where a_{m_1} , b_{m_2} , and c_{m_3} are the m_1 th, m_2 th, and m_3 th element of $\mathbf{a}^{(2)}$, $\mathbf{b}^{(2)}$ and $\mathbf{c}^{(2)}$, respectively, and $m_i \in [1, \dots, 2Z+1]$ for $i \in [1, 2, 3]$.

Thus, compared to $\Psi(\mathbf{a}^{(1)}, \mathbf{b}^{(1)}, \mathbf{c}^{(1)})$, the entries of $\Psi(\mathbf{a}^{(2)}, \mathbf{b}^{(2)}, \mathbf{c}^{(2)})$ are closer to the true components of the jammer signals. Similar to (6), the IF estimation with a higher accuracy can be achieved by solving

$$\min \left\| \mathbf{r}^{(2)} \right\|_1 \quad \text{s.t.} \quad \left\| \bar{\mathbf{y}} - \Psi(\mathbf{a}^{(2)}, \mathbf{b}^{(2)}, \mathbf{c}^{(2)}) \mathbf{r}^{(2)} \right\|_2^2 < \varepsilon. \quad (8)$$

Such iterations can be repeated until the required accuracy is obtained, or when the maximum number of iterations is achieved.

IV. JAMMER SUPPRESSION ALGORITHM

After the phases of all jammer signals are estimated, the jammer signals can be reconstructed using the estimated phase values while the corresponding magnitudes can be obtained from values of non-zero elements of sparse vector $\hat{\mathbf{r}}$. Then, the reconstructed j th jammer signal can be expressed as

$$\tilde{s}_j(t) = \tilde{\alpha}_j \exp(j\tilde{\varphi}_j(t)), \quad (9)$$

where $\tilde{\alpha}_j$ is the j th non-zero element of the estimated sparse vector $\hat{\mathbf{r}}$.

After the jammer signals are reconstructed, the subspace of the jammer signals can be expressed as

$$\mathbf{V} = [\mathbf{v}_1, \dots, \mathbf{v}_{Q_j}], \quad (10)$$

where $\mathbf{v}_j = [\tilde{s}_j(t_1), \dots, \tilde{s}_j(t_N)]^T$ for $j = 1, \dots, Q_j$. Thus, the projection matrix into the orthogonal subspace of the jammers is given by [11]

$$\mathbf{P} = \mathbf{I}_N - \mathbf{V}(\mathbf{V}^H \mathbf{V})^{-1} \mathbf{V}^H. \quad (11)$$

Then, the jammer-suppressed time-domain samples is obtained as

$$\hat{\mathbf{y}} = \mathbf{P}\bar{\mathbf{y}}. \quad (12)$$

V. SIMULATION RESULTS

In this section, simulation results are provided to verify the effectiveness of the proposed algorithm. As an example of the DS/SS signal, we consider an L1 band GPS signal ($Q_s = 1$) with the C/A code together with two nonstationary jammer signals ($Q_j = 2$) that imping at a GPS receiver. The signal-to-noise ratio (SNR) of the GPS waveform is set as -16 dB, and the jammer-to-noise ratio (JNR) of both jammer signals is assumed to be 25 dB unless otherwise specified.

The sampling frequency of the GPS receiver is set at the chip rate of the GPS signal, i.e., $f_s = 1.023$ MHz. The normalized IF laws of the two nonstationary jammers are set as

$$\begin{aligned}f_1(t) &= 0.1(t/G)^2 + 0.05(t/G) + 0.03, \\ f_2(t) &= 0.12(t/G)^2 + 0.15(t/G) + 0.13,\end{aligned}\quad (13)$$

for $t \in [0, \dots, G-1]$, and the number of total observations is set as $G = 256$ samples. The candidate of \mathcal{S} is assumed as $|\mathcal{S}| = 128$, i.e., 50% of samplings are missing.

Two different situations are considered. In the first case, the missing samples are randomly distributed with a uniform distribution. In the second case, the missing samples are located in several contiguous regions.

For the proposed method, the same procedure is applied in both situations. Three rounds of ℓ_1 -norm minimization are executed. In the first round, vectors $\mathbf{a}^{(1)}$, $\mathbf{b}^{(1)}$, $\mathbf{c}^{(1)}$ are set as uniformly sampled grids between 0 to 0.2 with step size 4×10^{-3} . In the second round, we set the step sizes as $\Delta a^{(2)} = \Delta b^{(2)} = \Delta c^{(2)} = 4 \times 10^{-4}$, whereas in the third round, $\Delta a^{(3)} = \Delta b^{(3)} = \Delta c^{(3)} = 4 \times 10^{-5}$ is used. $Z = 20$ is assumed in the last two rounds.

A. Random Missing Samples

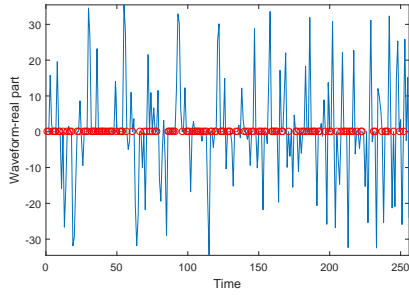
In Fig. 1(a), we provide the real-part of the received signal waveform, where red dots represent the missing samples. The corresponding true IFs of the nonstationary signals are shown in Fig. 1(b). Affected by the missing data samples, the Wigner-Ville distribution (WVD) [22, 23] is highly cluttered by the noise-like artifacts, and at the same time, it also suffers from the cross-terms, which make it difficult to estimate the IF of the jammer signal from this result.

The IF estimation results for the two nonstationary jammer signal are depicted in Fig. 2. It is shown that the IFs of the nonstationary jammers are estimated accurately.

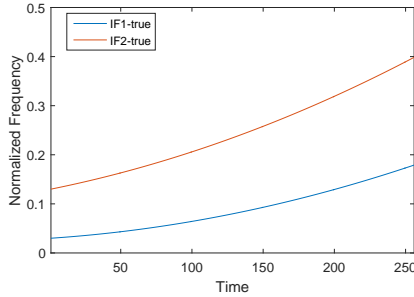
To quantitatively evaluate the performance, we use the root mean square error (RMSE) as the metric, defined as

$$\text{RMSE} = \sqrt{\frac{1}{Q_j} \sum_{j=1}^{Q_j} E[(\hat{f}_j(t) - f_j(t))^2]}, \quad (14)$$

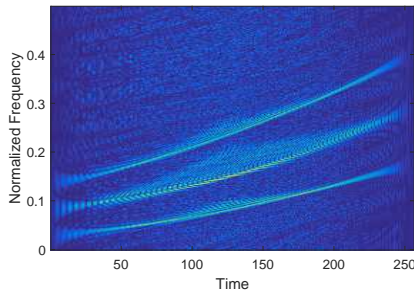
where \hat{f}_j denotes the estimate of the j th IF. Fig. 3 provides the RMSE of the IF estimation results compared with the non-parametric IF estimation method in [18]. From this result, we can see that the parametric method consistently outperforms the non-parametric sparse reconstruction approach.



(a) Waveform



(b) True IFs



(c) WVD

Fig. 1. Signal waveform, true IFs and TFD result with randomly missing samples.

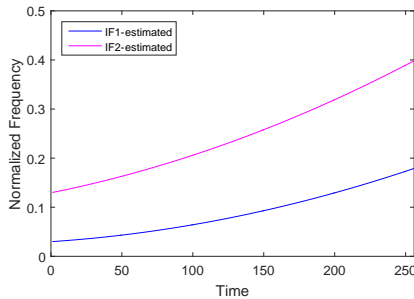


Fig. 2. IF estimation results.

The corresponding output SJNR, evaluated at the despread GPS symbol and averaged over the 50 independent trials, is depicted in Fig. 4. Compared with the non-parametric sparse reconstruction algorithm [18], the jammer suppression performance is highly improved by the proposed parametric estimation method.

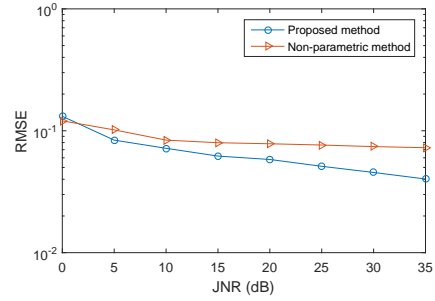


Fig. 3. Performance of the IF estimation method.

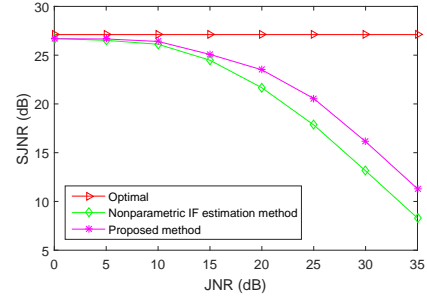


Fig. 4. Output SJNR versus input JNR.

B. Bursty Missing Samples

In the second case, data samples at the following positions are missing: sample 1, samples 34 to 67, samples 100 to 133, samples 166 to 213, and samples 246 to 256. The real-part waveform and the WVD are shown in Fig. 5. Figs. 6(a) and 6(b) provide the IF estimation result using non-parametric algorithm and the proposed parametric algorithm, respectively. It is clear that, in this case, the non-parametric approach fails to obtain the jammer IF signatures, whereas reliable jammer IF signatures are obtained from the proposed parametric approach.

VI. CONCLUSION

In this paper, we proposed a nonstationary jammer suppression technique for signals with missing samples based on parametric sparse reconstruction. In order to improve the jammer IF estimation accuracy and reduce the computational complexity, a data-dependent parametric dictionary matrix was designed. After multiple rounds of parametric sparse reconstruction processes, accurate jammer phase estimation is achieved to reconstruct the jammer signals. Effective jammer suppression were performed by applying the orthogonal projection technique.

REFERENCES

- [1] L. B. Milstein, "Interference rejection techniques in spread spectrum communications," *Proc. IEEE*, vol. 76, no. 6, pp. 657–671, June 1988.
- [2] J. D. Laster and J. H. Reed, "Interference rejection in digital wireless communications," *IEEE Signal Process. Mag.* vol. 14, no. 3, pp. 37–62, May 1997.
- [3] A. Leshem and A.-J. van der Veen, "Radio-astronomical imaging in the presence of strong radio interference," *IEEE Trans. Inform. Theory*, vol. 46, no. 5, pp. 1730–1747, Aug. 2000.

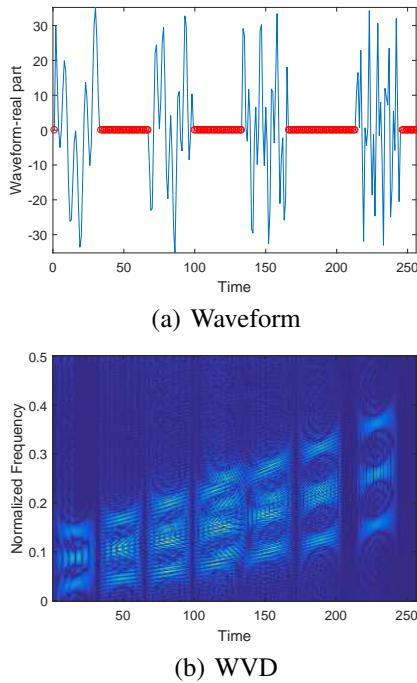


Fig. 5. Signal waveform and TFD result with bursty missing samples.

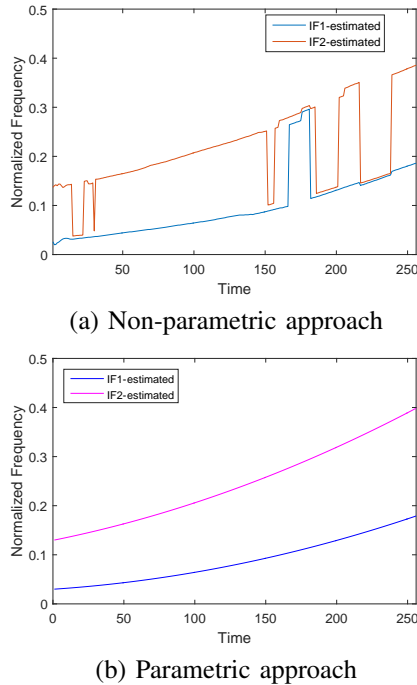


Fig. 6. Estimated jammer IFs from non-parametric and parametric approaches.

[4] M. G. Amin and Y. Zhang, "Interference suppression in spread spectrum communication systems," in J. G. Proakis (ed.), *The Wiley Encyclopedia of Telecommunications*. John Wiley, 2002.

[5] Y. D. Zhang and M. G. Amin, "Anti-jamming GPS receiver with reduced phase distortions," *IEEE Signal Process. Lett.*, vol. 19, no. 10, pp. 635-638, Oct. 2012.

[6] Y. Ye, D. Wu, Z. Shu, and Y. Qian, "Overview of LTE spectrum sharing technologies," *IEEE Access*, vol. 4, pp. 8105-8115, Nov. 2016.

[7] A. Hassaniien, M. G. Amin, Y. D. Zhang, and F. Ahmad, "Dual-function radar-communications: Information embedding using sidelobe control and waveform diversity," *IEEE Trans. Signal Process.*, vol. 64, no. 8, pp. 2168-2181, April 2016.

[8] B. Li, A. P. Petropulu, and W. Trappe, "Optimum co-design for spectrum sharing between matrix completion based MIMO radars and a MIMO communication system," *IEEE Trans. Signal Process.*, vol. 64, no. 17, pp. 4562-4575, May 2016.

[9] A. Hassaniien, M. G. Amin, Y. D. Zhang, and F. Ahmad, "Signaling strategies for dual-function radar communications: An overview," *IEEE Aerospace Electron. Syst. Mag.*, vol. 31, no. 10, pp. 36-45, Oct. 2016.

[10] Y. Zhang, M. G. Amin, and A. R. Lindsey, "Anti-jamming GPS receivers based on bilinear signal distributions," in *Proc. IEEE Military Communications Conf.*, Vienna, VA, Oct. 2001, pp. 1070-1074.

[11] Y. Zhang and M. G. Amin, "Array processing for nonstationary interference suppression in DS/SS communications using subspace projection techniques," *IEEE Trans. Signal Process.*, vol. 49, no. 12, pp. 3005-3014, Dec. 2001.

[12] M. G. Amin and Y. D. Zhang, "Nonstationary jammer excision for GPS receivers using sparse reconstruction techniques," in *Proc. ION GNSS+*, Tampa, FL, Sept. 2014, pp. 3469-3474.

[13] Y. D. Zhang, M. G. Amin, and B. Himed, "Reduced interference time-frequency representations and sparse reconstruction of undersampled data," in *Proc. European Signal Process. Conf.*, Marrakech, Morocco, Sept. 2013.

[14] L. Stankovic, S. Stankovic, I. Orovic, and Y. D. Zhang, "Time-frequency analysis of micro-Doppler signals based on compressive sensing," in M. Amin (ed.), *Compressive Sensing for Urban Radars*, CRC Press, 2014.

[15] Q. Wu, Y. D. Zhang, and M. G. Amin, "Continuous structure based Bayesian compressive sensing for sparse reconstruction of time-frequency distributions," in *Proc. Int. Conf. Digital Signal Process.*, Hong Kong, China, Aug. 2014, pp. 831-835.

[16] M. G. Amin, B. Jakonovic, Y. D. Zhang, and F. Ahmad, "A sparsity-perspective to quadratic time-frequency distributions," *Digital Signal Process.*, vol. 46, pp. 175-190, Nov. 2015.

[17] Y. D. Zhang, B. Wang, and M. G. Amin, "Multi-sensor excision of sparsely sampled nonstationary jammers for GPS receivers," in *Proc. ION GNSS+*, Tampa, FL, Sept. 2015, pp. 3284-3288.

[18] Y. D. Zhang, M. G. Amin, and B. Wang, "Mitigation of sparsely sampled nonstationary jammers for multi-antenna GNSS receivers," in *Proc. IEEE ICASSP*, Shanghai, China, March 2016.

[19] B. Wang, Y. D. Zhang, S. Qin and M. G. Amin, "Robust nonstationary jammer mitigation for GPS receivers with instantaneous frequency error tolerance," in *Proc. SPIE Compressive Sensing Conference*, Baltimore, MD, April 2016.

[20] D. Malioutov, M. Cetin, A. S. Willsky, "A sparse signal reconstruction perspective for source localization with sensor arrays," *IEEE Trans. Signal Process.*, vol. 53, no. 8, pp. 3010-3022, Aug. 2009.

[21] P. Flandrin and P. Borgnat, "Time-frequency energy distributions meet compressed sensing," *IEEE Trans. Signal Proc.*, vol. 58, no. 6, pp. 2974-2982, 2010.

[22] L. Cohen, *Time-Frequency Analysis*. Prentice Hall, 1995.

[23] B. Boashash (ed.), *Time-Frequency Signal Analysis and Processing*, 2nd Ed., Academic Press, 2015.

[24] J. A. Tropp and A. C. Gilbert, "Signal recovery from partial information via orthogonal matching pursuit," *IEEE Trans. Info. Theory*, vol. 53, no. 12, pp. 4655-4666, 2007.

[25] R. Tibshirani, "Regression shrinkage and selection via the Lasso," *J. Royal Statist. Soc.*, vol. 58, no. 1, pp. 267-288, 1996.

[26] S. Ji, D. Dunson, and L. Carin, "Multi-task compressive sampling," *IEEE Trans. Signal Process.*, vol. 57, no. 1, pp. 92-106, 2009.

[27] Q. Wu, Y. D. Zhang, M. G. Amin, and B. Himed, "Complex multitask Bayesian compressive sensing," in *Proc. IEEE ICASSP*, Florence, Italy, May 2014.